Identifying Dominant Phenomena in the Dose-Distance Curve for Optimization of Japanese Emergency Planning

Kodai Wadayama[a,b], Takafumi Narukawa[c], Takashi Takata[d], Yoshiyuki Narumiya[e], and Retsu Kojo[f]

[a] The University of Tokyo, 7-3-1 Hongo, Bunkyo-ku, Tokyo, 113-8656, wadayama@nse.t.u-tokyo.ac.jp

[b] Nuclear Regulation Authority, 1-9-9, Roppongi, Minato-ku, Tokyo, 106-8450, wadayama_kodai_pt7@nra.go.jp

[c] The University of Tokyo, 7-3-1 Hongo, Bunkyo-ku, Tokyo, 113-8656, narukawa@n.t.u-tokyo.ac.jp

[d] The University of Tokyo: 7-3-1 Hongo, Bunkyo-ku, Tokyo, 113-8656, takata_t@n.t.u-tokyo.ac.jp

[e] The University of Tokyo: 7-3-1 Hongo, Bunkyo-ku, Tokyo, 113-8656, ynarumiya@n.t.u-tokyo.ac.jp

[f] Nuclear Regulation Authority, 1-9-9, Roppongi, Minato-ku, Tokyo, 106-8450, kojo_retsu_px2@nra.go.jp

Abstract: Understanding the dose-distance curve is essential for determining the emergency planning zone. The variation of dose with distance is affected by a combination of multiple phenomena, each following either a power-law or an exponential decay law. In our previous study, we examined the range of applicability of the power law by focusing on various accident scenarios and meteorological conditions. However, further investigation is needed to clarify the dominant phenomenon under different conditions. Therefore, the objective of this study is to clarify the relative importance of each phenomenon depending on the conditions. For accident scenarios, containment failure, and filtered containment venting were considered. For meteorological conditions, 8,760 cases were analyzed using one year of site data from Japan. In addition, release height and finite cloud correlation factors, which were not addressed in the previous study, were incorporated as parameters herein. For the identification of phenomenon importance, distance semi-elasticity was introduced as an indicator, that quantifies the relative change in dose per unit increase in distance. In most cases, atmospheric dispersion, characterized by power-law attenuation, was the dominant factor controlling distance-dependent attenuation. Nevertheless, in some cases, exponential-law components exerted an effect comparable to that of the dispersion term, such as under certain rainfall conditions at a far distance. Because the influence of the dispersion term described by a power-law form diminishes with increasing distance, exponential terms such as depletion by deposition can become dominant at larger distances in some cases. However, for evaluations up to approximately 30 km, such meteorological patterns were not frequently observed. Thus, from a statistical perspective, the dispersion term remained dominant overall. Based on these findings, a decision-making framework for determining the emergency planning zone was proposed. The power law describes the scaling relationship between distance and dose supporting decision-making for defining the emergency planning zone based on proportional changes in reactor thermal power. In contrast, under a power law, the change in dose per unit distance diminishes with increasing distance, implying that the marginal benefit of moving an additional unit distance decreases as one moves farther away.

1. INTRODUCTION

Emergency Planning Zone (EPZ) is an area in which protective actions are predefined and prepared in advance to enable rapid protective action for residents in the event of a nuclear emergency [1–3]. In recent years, the development of advanced nuclear reactors has accelerated, increasing the need for research into novel methodologies for EPZ determination that consider reactor-specific risk characteristics [4]. Although various approaches to EPZ determination have been proposed, an essential element of this process is the evaluation of dose–distance (D–D) curves, which represent radiation dose as a function of distance for a given accident scenario. In particular, the relative shape of the D–D curve provides critical information for determining appropriate EPZ boundaries [5].

Previous studies on the shape of dose–distance (D–D) curves can be summarized as follows. NUREG-0396 proposed a method for representing D–D curves using a power-law form, $1/r^n$ for the Design Basis Accident (DBA) scenario [6]. Building on this work, the authors have previously conducted scenario-based analyses to further clarify the characteristics of D–D curves. In our previous study, it was demonstrated that under rainfall conditions, the shape of the D–D curve varies depending on the accident scenario, based on the aerosol contribution to dose [7]. Furthermore, the authors previously investigated that the meteorological conditions under consideration were expanded to examine the range of conditions over which the power-law approximation remains applicable [8].

These studies have discussed the shape of the D–D curve in relation to nuclide composition and aerosol fraction to effective dose. However, decision-making based on D–D curves require not only the qualitative understanding of their shapes but also the elucidation of the underlying governing mechanisms. The shape of a D–D curve is affected by several phenomena, each of which can often be described by either a power-law or an exponential-law. Examples include the effect of atmospheric dispersion, which is commonly approximated by a power-law, as well as nuclide radioactive decay and plume concentration depletion caused by deposition, which can be expressed in forms close to exponential attenuation.

Nevertheless, to the best of our knowledge, previous studies have not examined the relative dominance of these phenomena—that is, which processes primarily govern the distance-dependent attenuation of D–D curves—while considering the actual site-specific meteorological conditions. This remains an important unresolved issue. Accordingly, the objectives of the present study are as follows:

- To quantitatively clarify which of the following phenomena substantially contributes to distance-dependent attenuation: wet deposition (exponential attenuation), dry deposition (exponential attenuation), or atmospheric dispersion (power-law attenuation).
- To evaluate whether the change in dose with distance follows an exponential or power-law behaviour under annual meteorological conditions at a site in Japan.

A particularly important feature of the present study is that the analysis was based not merely on a limited set of meteorological data but on a full range of meteorological conditions over one year at actual Japanese site. This enabled the systematic determination of the phenomena under which conditions.

2. PHENOMENON AFFECTING THE D-D CURVE

The phenomena affecting D–D curves are described below.

(1) Atmospheric dispersion
Atmospheric dispersion describes the transport and spreading of a plume by atmospheric motion, whereby the plume expands in the horizontal (y-axis) and vertical (z-axis) directions, and its concentration decreases with increasing distance from the source. In calculations of groundshine and inhalation dose, the effect of dispersion is evaluated using the relative concentration, $D_{\chi/Q}(x)$. Over relatively short ranges, this behavior is commonly represented using the Gaussian plume model [9] as follows:

$$D_{\chi/Q}(x)=\frac{1}{2\pi\sigma_y\sigma_z u}\exp\left(-\frac{y^2}{2\sigma_y^2}\right)\left(\exp\left(-\frac{(z+h)^2}{2\sigma_z^2}\right)+\exp\left(-\frac{(z-h)^2}{2\sigma_z^2}\right)\right) \quad (1)$$

where u is the wind speed and h is the release height. Dispersion parameters, σ_y and σ_z, are approximately proportional to the power of downwind distance x. In SOARCA analyses, σ_y and σ_z

are represented as nearly proportional to a power of x [10], and a similar approach—under which they are treated as being nearly proportional to a power of x—is also adopted in the Japanese meteorological guidelines [11]. Therefore, the denominator may be considered a power-law term.

The exponential term on the right-hand side represents the effects of vertical distribution and ground reflection. Because this term is in a negative exponential form, a greater release height tends to reduce the concentration in the vicinity of the source. However, as the distance increases, the effect of this term decreases and asymptotically approaches an approximately constant value of unity.

In the evaluation of cloudshine dose, the dispersion effect is reflected in the relative dose, $D_{\chi/Q}(x)$, by multiplying the centerline concentration by a plume correction factor $C(x)$ [12] as follows:

$$D_{D/Q}(x) = D_{\chi/Q}^{centerheight}(x) \times C(x) \qquad (2)$$

The relative dose, $D_{D/Q}(x)$, deviates from $D_{\chi/Q}(x)$ near the release source (approximately several hundred meters to 1 km), whereas at longer distances, it becomes nearly identical to $D_{\chi/Q}(x)$.

(2) Radioactive decay during atmospheric dispersion
This process corresponds to the radioactive decay of nuclides during atmospheric dispersion as follows:

$$D_{decay}(x) = \exp(-\lambda_i \frac{x}{u}) \qquad (3)$$

Within the Gaussian plume model, plume transport is assumed to occur along a straight path; accordingly, the decay time is taken to be the downwind distance x divided by the wind speed u. The λ_i is decay coefficient of nuclide i.

(3) Dry deposition:
Although deposition increases groundshine dose, it simultaneously reduces the concentration of radioactive materials in the plume. In terms of the distance dependence of the effective dose, the important effect is the depletion of nuclides in the plume, which contributes to the attenuation of the effective dose with distance [12]. The corresponding equation of dry deposition depletion is as follows:

$$D_{dry}(x) = \exp\left[-\sqrt{\frac{2}{\pi}} \frac{V_d}{u} \int_0^x \frac{1}{\sigma_z(x')} \left(-\frac{h^2}{2\sigma_z^2(x')} \right) dx' \right] \qquad (4)$$

where V_d is the dry deposition velocity, applied to aerosol nuclides and inorganic iodine species. A typical value of V_d is around 0.3 cm/s [13]. Deposition velocities for noble gases and organic iodine are often not accounted for [14].

(4) Wet deposition:
As in the case of dry deposition, wet deposition contributes to an increase in groundshine dose, whereas from the standpoint of the D–D curve, it reduces the effective dose with increasing distance. This dose reduction is represented through attenuation by a washout coefficient Λ, as following equation.

$$D_{wet} = \exp(-\Lambda \frac{x}{u}) \qquad (5)$$

Wet deposition differs from the other processes in that it occurs only during precipitation events. In NUREG-1150, the washout coefficient is assumed to be given by the following expression for all nuclides other than gaseous species [13]:

$$\Lambda = 9.5\times10^{-5} R^{0.8} \qquad (6)$$

where R is the rain intensity, and Λ is the washout coefficient. Herein, a uniform Λ value was assumed for all depositable nuclides, whereas $\Lambda = 0$ was used for noble gases and organic iodine. As discussed in our previous study [8], the effective dose was calculated as follows. First, the quantity of released radioactive materials was estimated using the source-term calculation method. This quantity was then multiplied, for each nuclide, by the dispersion term and the deposition/depletion term. Finally, the exposure dose, $E(x)$, was obtained by applying the dose conversion factor [15**,** 16] for each nuclide.

$$\begin{aligned} E(x) &= E_{CS} + E_{GS} + E_{IH} \\ &= D_{D/Q}(x)\sum_i \left(K_i^{CS} Q_i D_{decay}(x) D_{wet}(x) D_{dry}(x) \right) \\ &+ D_{\chi/Q}(x)\sum_i \left(K_i^{IH} Q_i D_{decay}(x) D_{wet}(x) D_{dry}(x) \right) \\ &+ D_{\chi/Q}(x)\sum_i \left(K_i^{GS} Q_i D_{decay}(x) D_{wet}(x) D_{dry}(x)(V_d + V_R) \right) \end{aligned} \qquad (7)$$

where K_i^{CS}, K_i^{GS}, and K_i^{IH} are the dose conversion factors of cloudshine, groundshine, and inhalation dose, respectively; Q_i is the released fission product (FP), V_d is the dry deposition velocity, and V_R is the wet deposition rate.

3. QUANTIFICATION OF PHENOMENON IMPORTANCE USING SEMI-ELASTICITY

Semi-elasticity is defined as the percentage change in $E(x)$ resulting from an infinitesimal change in x and is widely used in the field of economics. In this study, distance semi-elasticity is introduced as an indicator for quantitatively evaluating the relative importance of the phenomena described in Section 2. It can be interpreted as the rate of change in dose with respect to distance described as follows:

$$\eta = \frac{d\log(E(x))}{dx} = \frac{1}{E(x)}\frac{dE(x)}{dx} \qquad (8)$$

The phenomenon described in Section 2 affects only specific nuclides. Using the term $E_j(x)$ for the group of radionuclides influenced by phenomenon *j*, Equation (8) can be rewritten as follows:

$$\eta = \frac{d\log\left(E(x)\right)}{dx} = \frac{E_j(x)}{E(x)}\frac{d\log\left(E_j(x)\right)}{dx} + \frac{E(x)-E_j(x)}{E(x)}\frac{d\log\left(E(x)-E_j(x)\right)}{dx} \qquad (9)$$

A major advantage of using distance semi-elasticity lies in its ability to isolate the specific contribution of distance decay ***j.*** By leveraging logarithmic transformation, multiplicative relationships are converted into additive components, making this new approach effective for Phenomenon Identification and Ranking. Initially, we extract the semi-elasticity associated with the $E_j(x)$ term. $E_j(x)$ is the product of the term $D_j(x)$, representing the distance decay phenomenon *j* of interest, the term $O(x)$ for other distance decay effects, and the distance-independent term *N* in light of Equation (7). This multiplicative relationship can be converted into an additive one as follows:

$$\frac{E_j(x)}{E(x)}\frac{d\log\left(E_j(x)\right)}{dx} = \frac{E_j(x)}{E(x)}\left(\frac{d\log\left(D_j(x)\right)}{dx} + \frac{d\log\left(O(x)\right)}{dx} + \frac{d\log\left(N\right)}{dx} \right) \qquad (10)$$

Finally, the semi-elasticity related to the phenomenon of interest $\mu_{D_j,weighted}$, can be extracted as follows:

$$\eta_{D_j,weighted} = \frac{E_j(x)}{E(x)} \frac{d\log\left(D_j(x)\right)}{dx} \qquad (11)$$

Herein, parameter $\eta_{D_j,weighted}$ was used to compare the importance of different phenomena. In the present study, the semielasticity of the dispersion term was calculated as the sum of the semi-elasticity of $D_{D/Q}(x)$ weighted by the contribution of cloudshine to the effective dose and the semi-elasticity of $D_{\chi/Q}(x)$ weighted by the contributions of inhalation and groundshine to the effective dose.

4. ANALYSIS CONDITIONS

The accident scenarios analyzed in this study were the same as those considered in previous studies [7, 8], namely:
CF-24h, corresponding to containment failure at 24 hours;
FV-24h, corresponding to filtered venting at 24 hours. They are shown in Table 1.

Table 1: Accident Scenarios Considered in This Study

Accident scenario	Description of the accident scenario	Xe release fraction	I release fraction	Cs release fraction	Te release fraction
CF-24h (small mitigation)	Core melt and release of FP to the environment 24 h after reactor shutdown due to containment failure	9.5E−01	7.9E−03	6.0E−03	1.5E−03
FV-24h (large mitigation)	Core melt and release of FP to the environment 24 h after reactor shutdown due to filtered containment venting	9.5E−01	8.0E−06	3.0E−07	7.5E−08

By considering accident scenarios with different aerosol contributions to dose, the dominant phenomena affecting distance-dependent attenuation can be quantitatively characterized for each scenario using semi-elasticity. For meteorological conditions, 8,760 cases (corresponding to one year of hourly = 365 days × 24 h) of numerical weather data from the Mesoscale Model Grid Point Value around a representative site on the Pacific coast of Japan were used [17]. Numerical weather data from the Mesoscale Model Grid Point Value (GPV) were processed using methodologies adopted in a previous study [18] to make them suitable for Gaussian plume calculations. These data are presented in Figure 1.

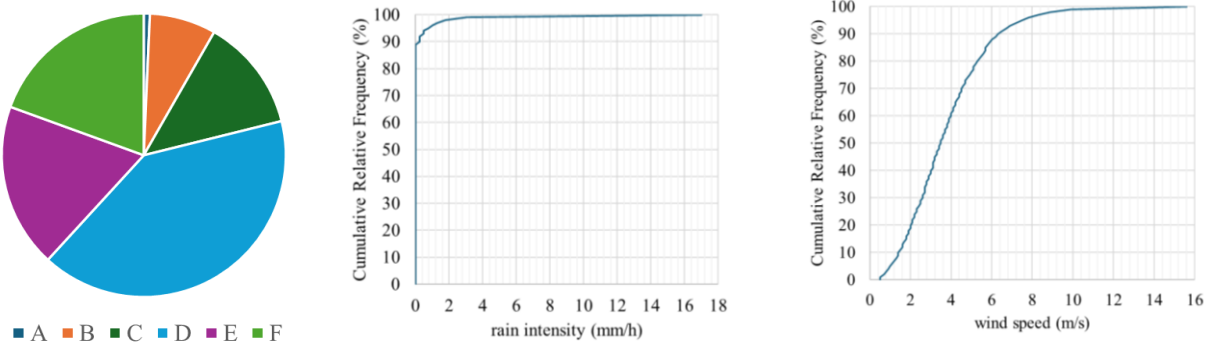

Figure. 1. Meteorological Conditions at the Target Site
(from Left to Right: Atmospheric Stability, Precipitation, and Wind Speed Distributions)

The meteorological characteristics of the site were as follows. For stability, class D was the most frequently observed; however, stable and unstable conditions were relatively well balanced overall. Precipitation occurred during about 10% of the year. Wind speeds were primarily distributed within 2–5 m/s.

5. RESULTS AND DISCUSSION

5.1. Comparison of Dominant Phenomena among Accident Scenarios Using Semi-Elasticity

In the following, the semi-elasticities of the four components—atmospheric dispersion, dry deposition, wet deposition, and radioactive decay during atmospheric dispersion—are presented for the two scenarios (CF-24h and FV-24h). This allows the evaluation of the relative contributions of these phenomena to distance-dependent attenuation. The distance semi-elasticity was first evaluated at the 2 km location, corresponding to the vicinity of the plant. The results are shown in Figure 2.

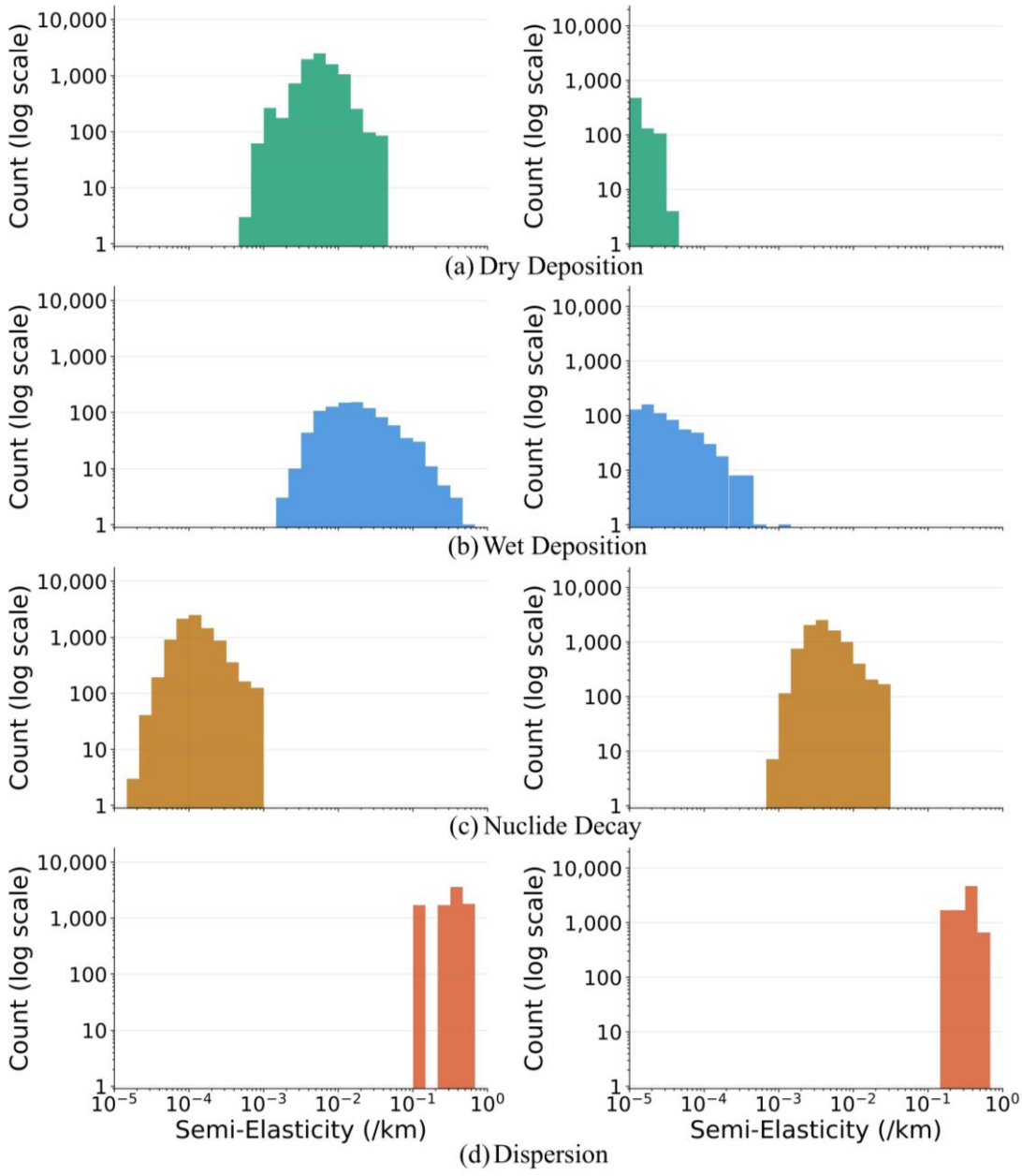

Figure 2: Semi-Elasticity Comparison by Phenomenological Component

As shown in Figure 2, the overall distribution trend for the containment failure scenario indicates that the semi-elasticities decrease in the following order: (d) dispersion > (b) wet deposition (in some cases) > (a) dry deposition > (c) nuclide decay.

The large contribution of the dispersion term was attributed to the focus of the analysis on the near field. In other words, because the dispersion term is strongly governed by a power-law, the change per unit distance is greater at shorter distances.

The second most influential phenomenon is wet deposition caused by rainfall, with the shape of its distribution being of particular interest. Specifically, the semi-elasticity associated with wet deposition becomes large under certain conditions, such as extreme rainfall or low wind speeds, whereas its contribution remains small under light-rain conditions. Because the wet deposition term is sensitive to both wind speed and precipitation intensity, its distribution spans a wide range. However, the number of precipitation cases is approximately an order of magnitude smaller than that for the other phenomena because rainy conditions occur less frequently overall. In this sense, if occurrence frequency is also considered, the overall importance of wet deposition becomes relatively limited.

The contribution of the semi-elasticity associated with dry deposition is the third largest and approximately one to two orders of magnitude smaller than that of the dispersion term. Assuming a typical dry deposition velocity for representative severe-accident aerosol particle sizes (approximately 0.3 cm/s) [13], these results suggest that plume depletion caused by dry deposition is not an influential phenomenon. However, it should be noted that dry deposition can occur under any meteorological conditions throughout the year, unlike wet deposition. The variations among meteorological cases were primarily attributed to wind speed and atmospheric stability. In particular, lower wind speeds lead to a larger effect of dry deposition depletion.

Finally, radioactive decay during atmospheric dispersion shows only a limited effect. This is because iodine nuclides that dominate the containment failure scenario, such as I-131 (half-life: 8 days), undergo very little decay over atmospheric transport times (only a few hours).

For the filtered containment venting scenario, the semi-elasticities decrease as follows: (d) atmospheric dispersion > (c) nuclide decay > (b) wet deposition under some precipitation cases > (a) dry deposition.

These results indicate that deposition has only a minor effect on overall distance-dependent attenuation because aerosol nuclides subject to deposition account for only a small fraction of the effective dose. The semi-elasticity associated with deposition is less than 0.1% per kilometer, meaning that even a 1-km increase in distance reduced the dose contribution by less than 0.1%. Thus, the effect of deposition can be considered extremely small.

As the effect of deposition diminishes, the relative contribution of nuclide decay becomes more pronounced. This was attributed to the impact of short-lived noble-gas nuclides. The shape of the distribution is very similar to that under the CF-24h scenario, presumably because wind speed is the only meteorological variable affecting radioactive decay during atmospheric dispersion. In other words, the distributional shape of the in-plume decay term is governed by the wind speed distribution, whereas the magnitude of the semi-elasticity itself depends on the nuclides that dominate the dose.

5.2. Sensitivity Analysis: Variation in Dominant Phenomena with Distance

Next, the variations of semi-elasticity with distance are discussed. As a representative example, the CF-24h case is presented, in which various components of the semi-elasticity were identified. Figure 3 compares the semi-elasticities at the 2 km and 25 km points.

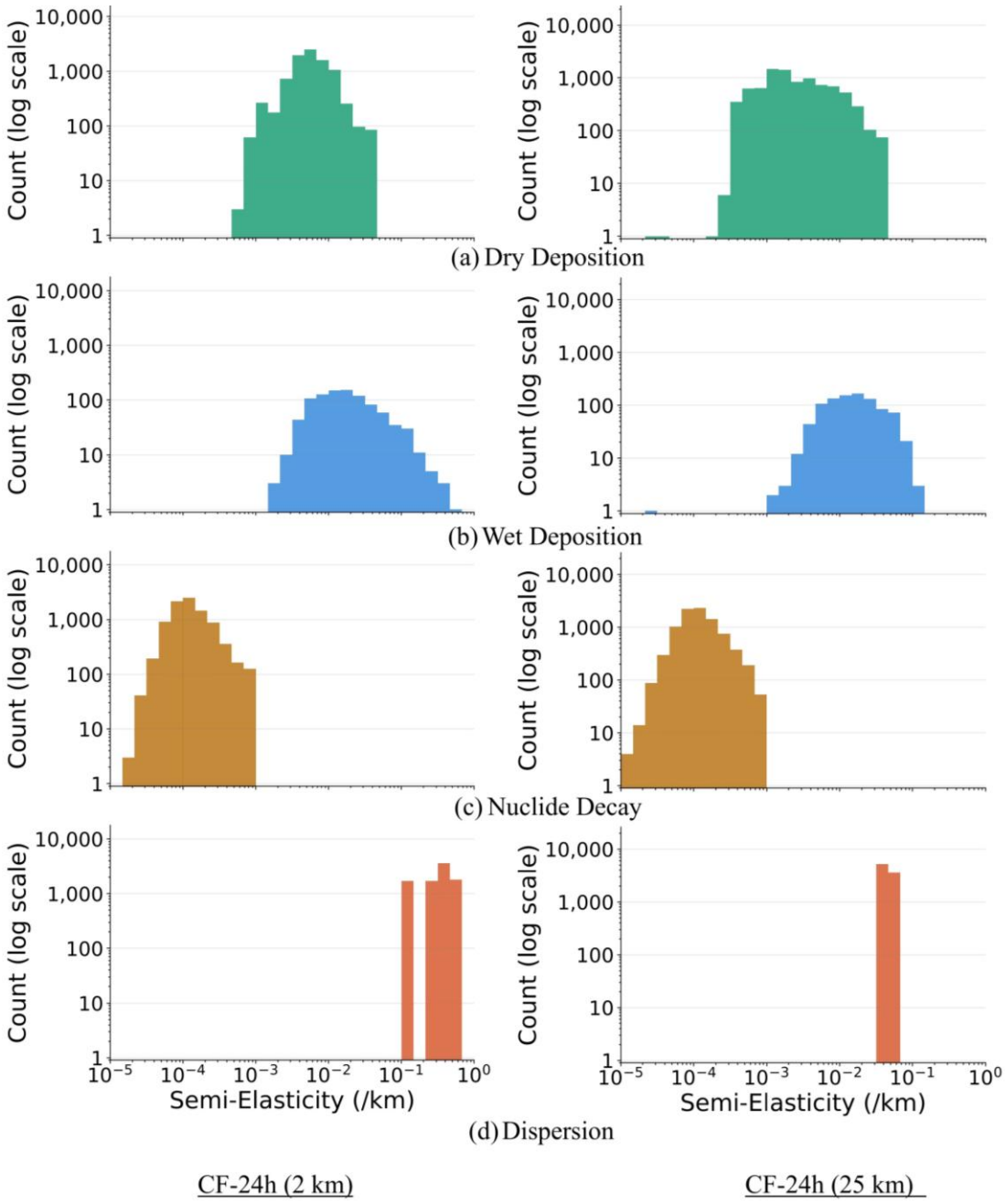

Figure 3: Semi-Elasticity Comparison by Distance

For wet deposition, dry deposition, and radioactive decay during atmospheric dispersion, little difference was observed between the semi-elasticities evaluated at 2 km and 25 km. In contrast, the semi-elasticity of the dispersion term at 25 km was approximately one order of magnitude smaller than that at 2 km. This suggests that, at 25 km, the precipitation-related term may in some cases become more important than the dispersion term in governing distance-dependent attenuation.

This behavior is consistent with the functional form of each term. Because the wet deposition term is expressed as an exponential function, its semi-elasticity is constant with respect to distance x.

On the other hand, because the dispersion term follows a power-law dependence, its semi-elasticity decreases in magnitude as distance increases. This explains why the semi-elasticity at 25 km is smaller approximately one order of magnitude than that at 2 km. Although the dispersion term remains

dominant over the precipitation term (and the dry-deposition term) at 25 km for most meteorological conditions, the dominant phenomenon may change if the evaluation distance is extended further.

Accordingly, within the relatively near-field range relevant to EPZ determination, atmospheric dispersion can reasonably be considered the dominant phenomenon.

5.3. Semi-Elasticity Averaged across All Meteorological Conditions

Figure 4 presents the overall mean semi-elasticity of the scenario, evaluated over all meteorological conditions. Figure 5 compares of the dispersion component semi-elasticity and the total semi-elasticity as functions of distance.

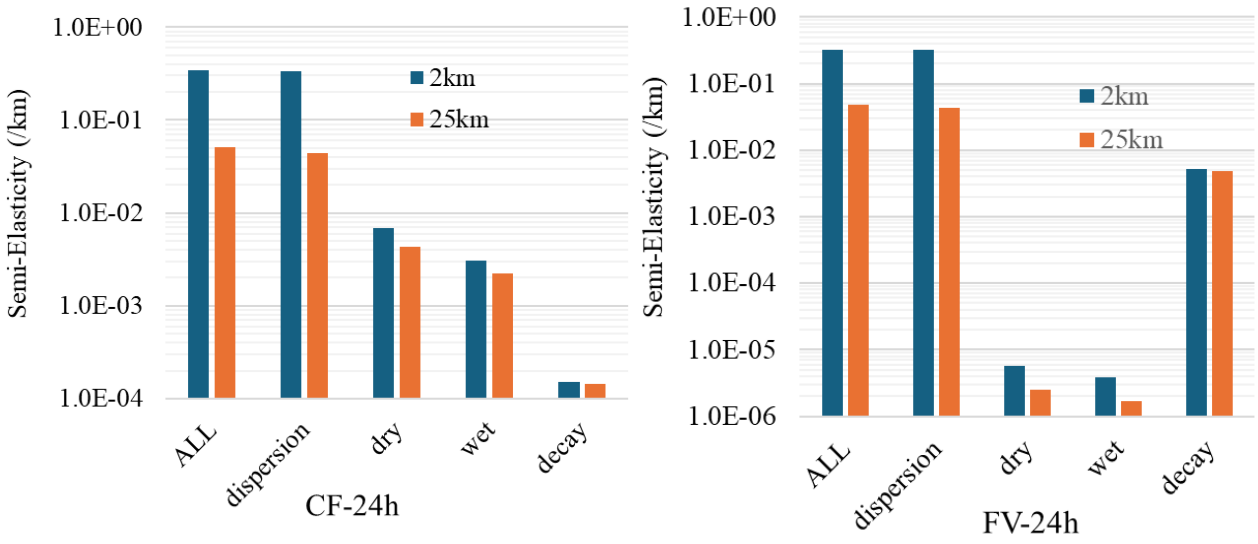

Figure 4: Semi-Elasticity of each Component Averaged across All Meteorological Conditions

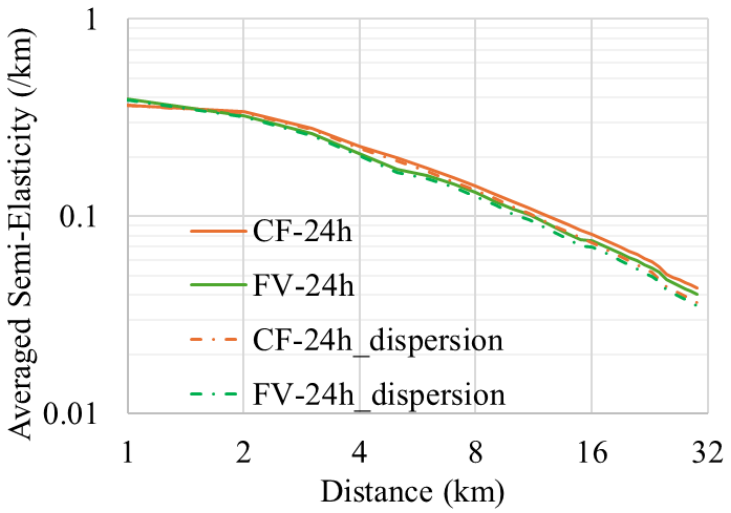

Figure 5: Semi-Elasticity of each Distance Averaged across All Meteorological Conditions

As shown in Figure 4, for both the CF-24h and FV-24h accident scenarios, the weather-averaged overall semi-elasticity of the entire scenario closely approximates the average semi-elasticity of the

dispersion component. In contrast, the averaged semi-elasticities of other components (dry deposition, wet deposition, and decay) are found to be orders of magnitude lower than that of dispersion. A notable observation is the semi-elasticity of wet deposition; while it exhibited high values during actual rainfall events, its weather-averaged value remained small.

Figure 5 suggests that, owing to the averaging effect, the mean semi-elasticity of the overall dose is almost entirely governed by the dispersion term. That is, when all meteorological conditions are considered collectively, the overall distance semi-elasticity is dominated by atmospheric dispersion.

An interesting implication is that the overall distance semi-elasticity may be represented by an approximately common form regardless of the accident scenario, because it is ultimately controlled by the dispersion semi-elasticity, which does not depend on nuclide composition. This may be regarded as one of the notable findings of this study.

6. DECISION-MAKING USING THE D-D CURVE

This section discusses how the results of the present study may contribute to EPZ determination and to the design of protective actions. A key finding is that, as shown in Figures 4 and 5, when averaged over all meteorological conditions, dispersion factor χ / Q (relative concentration), which exhibits power-law behavior, dominates the overall distance-dependent attenuation in the near field. In other words, for the site considered in this study, the average risk attenuation with distance is suggested to follow a power-law trend.

6.1. EPZ Scaling with Reactor Thermal Power

One possible application, which has also been discussed in previous studies [1,8], is the scaling of EPZ distance based on reactor thermal power. In general, the initial core inventory of FP is proportional to reactor thermal power. Additionally, if the accident scenario is assumed to be the same, the environmental release fraction to the core inventory is also the same. Under such conditions, the distance at which a given dose criteria are reached on the D–D curve is determined by the change in the initial FP inventory associated with reactor power. In cases where the D–D curve is well approximated by a power-law function such as $1/x^n$, the distance corresponding to a specified dose criterion is suggested to follow a simple scaling formula:

$$x_{target} = \left(\frac{P_{target}}{P_{ref}} \right)^{\frac{1}{n}} \times x_{ref} \qquad (12)$$

where x_{ref} is distance exceeding dose criteria at reference plant, x_{target} is distance exceeding dose criteria at target plant, P_{ref} is thermal power of reference plant, and P_{target} is thermal power of target plant. A major advantage of this expression is that, regardless of the specific dose limit selected or the accident scale assumed, distance x can be approximately scaled in proportion to the reduction in reactor power.

For example, if the D–D curve follows $1/x^2$ and reactor thermal power of the target plant is reduced to one quarter compared with that of reference plant, the distance at which the same dose is reached becomes one half.

6.2. Estimation of EPZ Distance and Protective Action Effectiveness Using Semi-Elasticity

Another possible application is the estimation of EPZ distance, and the effectiveness of protective actions based on semi-elasticity. If the D–D relationship is dominated by atmospheric dispersion, which follows a power-law, the semi-elasticity decreases with increasing distance. This means that the benefit of relocating by a fixed distance increment, Δx —namely, the effectiveness of evacuation—diminishes with increasing distance from the source. In situations where additional movement yields only a limited dose reduction, it may be more appropriate to prepare alternative protective actions, such as sheltering, rather than prioritizing evacuation. Overall, by analyzing semi-elasticity for each scenario at each distance, the present study determined which mechanisms—particularly power-law attenuation or exponential attenuation—dominate under given conditions. In this respect, the framework developed herein may provide a useful basis for EPZ-related decision-making.

At the same time, several limitations should be recognized. First, because the discussion in Section 6 is based on average behavior, the effects of extreme meteorological conditions may be smoothed out. Second, even in the case of $D_{\chi/Q}(x)$ or $D_{D/Q}(x)$, the very near field (for example, about 100 m) cannot necessarily be represented by a pure power-law curve due to building wake effect or plume rise.

Accordingly, the present framework should be regarded as most suitable for use in the initial stage of EPZ determination.

7. CONCLUSION

In this study, we introduced the concept of distance semi-elasticity as a novel indicator to establish a quantitative framework for evaluating the relative importance of phenomena affecting the dose–distance (D–D) curves. This framework enables the discrimination of cases in which power-law behavior is dominant from those in which exponential-law behavior is dominant.

Based on the actual annual site meteorological data, the phenomena exerting the greatest influence on D–D curves were analyzed. In the majority of cases, atmospheric dispersion, characterized by power-law attenuation, was the dominant factor controlling distance-dependent attenuation.

Nevertheless, in some cases, exponential-law components exerted an effect comparable to that of the dispersion term, such as under certain rainfall conditions at a far distance. Because the impact of the dispersion term (described by a power-law) diminishes with increasing distance, exponential terms, such as depletion by deposition, can become dominant at larger distances in some cases. However, for evaluations up to approximately 30 km, such meteorological patterns were not frequently observed. Thus, from a statistical perspective, the dispersion term remained dominant overall.

Accordingly, when EPZ determination is discussed on the basis of the all-meteorology-averaged D–D curve, power-law distance attenuation is suggested as a representative behavior.

If an ideal power-law relationship allows the representation of the D–D curve, and if the plants are of the same design type, EPZ can be evaluated using a scaling approach based on thermal power. In contrast, under a power-law, the change in dose per unit distance diminishes with increasing distance, implying that the marginal benefit of moving an additional unit distance decreases with increasing distance from the plant. This suggests that the benefit of relocating by a fixed distance increment—namely, the effectiveness of evacuation—diminishes with increasing distance from the source.

Acknowledgements
We gratefully thank Professor Emeritus. Yutaka Abe for giving grateful comments, and Dr. Chihiro Suzuki for providing the meteorological dataset for gaussian simulation derived from publicly available GPV data.

References

[1] M. Iivonen. "Review of SMR siting and emergency preparedness, Finland", VTT Technical Research Centre of Finland, VTT Research Report No. VTT-R-01612-20, (2022).

[2] J. C. de la Rosa Blul. “Determination of Emergency Planning Zones distances and scaling-based comparison criteria for downsized Nuclear Power Plants”, Nuclear Engineering and Design, Volume 382, 111367, (2021).

[3] S. I. Faisal, A. Ayoub, M. A. M. Soner, and M. S. Islam. “Deterministic assessment of emergency planning zones and radiological protective measures for Bangladesh’s VVER-1200 reactor under severe postulated events”, Nuclear Engineering and Design, Volume 433, 113841, (2025).

[4] F. C. V. Mancini, E. Gallego, and M. E. Ricotti. “Revising the Emergency Management Requirements for new generation reactors”, Progress in Nuclear Energy, 71 pp. 160-171, (2014).

[5] IAEA. “Actions to Protect the Public in an Emergency due to Severe Conditions at a Light Water Reactor”, International Atomic Energy Agency, 2013, Vienna.

[6] U.S. Nuclear Regulatory Commission. “Planning basis for the development of state and local government radiological emergency response plans in support of light water nuclear power plants”, NUREG-0396, U.S. Nuclear Regulatory Commission, 1978, Washington, DC.

[7] K. Wadayama, R. Kojo, T. Niisoe. “The effect of using Filtered Containment Venting System on variation in dose with distance in the prompt accident consequence assessment”, Journal of Nuclear Science and Technology, 61:9, pp. 1248–1264, (2024).

[8] K. Wadayama, R. Kojo, T. Narukawa, T. Takata. “STUDY ON A CONSEQUENCE-INFORMED DECISION MAKING FOR EMERGENCY PLANNING ZONE DISTANCE WITH DOSE VERSUS DISTANCE CURVE”, Asian Symposium on Risk Assessment and Management, 2025, Pattaya, Thailand.

[9] F. Pasquill, “The Estimation of the Dispersion of Windborne Material”, Meteorol.Mag.90, pp. 33–49, (1961).

[10] U.S. Nuclear Regulatory Commission. “State-of-the-Art Reactor Consequence Analyses (SOARCA)”, Vol. 1 (Rev. 1): Peach Bottom Integrated Analyses, and Vol. 2 (Rev. 1): Surry Integrated Analyses, NUREG/CR-7110, NRC, 2013, Washington, DC.

[11] Nuclear Safety Commission, Japan, 1982. “Meteorological guidance for reactor safety analysis” [in Japanese]

[12] A. J. Nosek, N. Bixler, 2021. “MACCS theory manual”, SAND2021-11535, Sandia National Laboratories, 2021, Albuquerque.

[13] U.S. Nuclear Regulatory Commission. “Severe accident risks: an assessment for five U.S. Nuclear power plants”, NUREG-1150, vol. 1, U.S. Nuclear Regulatory Commission, 1990,Washington, DC.

[14] J.V. Ramsdell, G.F. Athey, S.A. McGuire and L.K. Brandon. “RASCAL 4: description of models and methods”, NUREG-1940, U.S. Nuclear Regulatory Commission, 2012, Washington, DC.

[15] ICRP, “Compendium of Dose Coefficients based on ICRP Publication 60”. ICRP Publication 119. Ann. ICRP 41(Suppl.), (2012).

[16] ICRP. “Dose Coefficients for External Exposures to Environmental Sources”. ICRP Publication 144: Ann ICRP. 49(2):11-145, (2020).

[17] Meso Scale Model GPV (MSM) [Internet]. Japan Meteorological Business Support Center. 2022 June 16 [cited 2026 May 1]. Available from: https://www.jmbsc.or.jp/jp/online/file/f-online10200.html

[18] C. Suzuki. “Investigation of atmospheric stability classification methods using numerical weather data”. Journal of Nuclear Science and Technology, 62(11), 1135–1153, (2025).